SSCL-490

SSCL-490

Superconducting Super Collider Laboratory

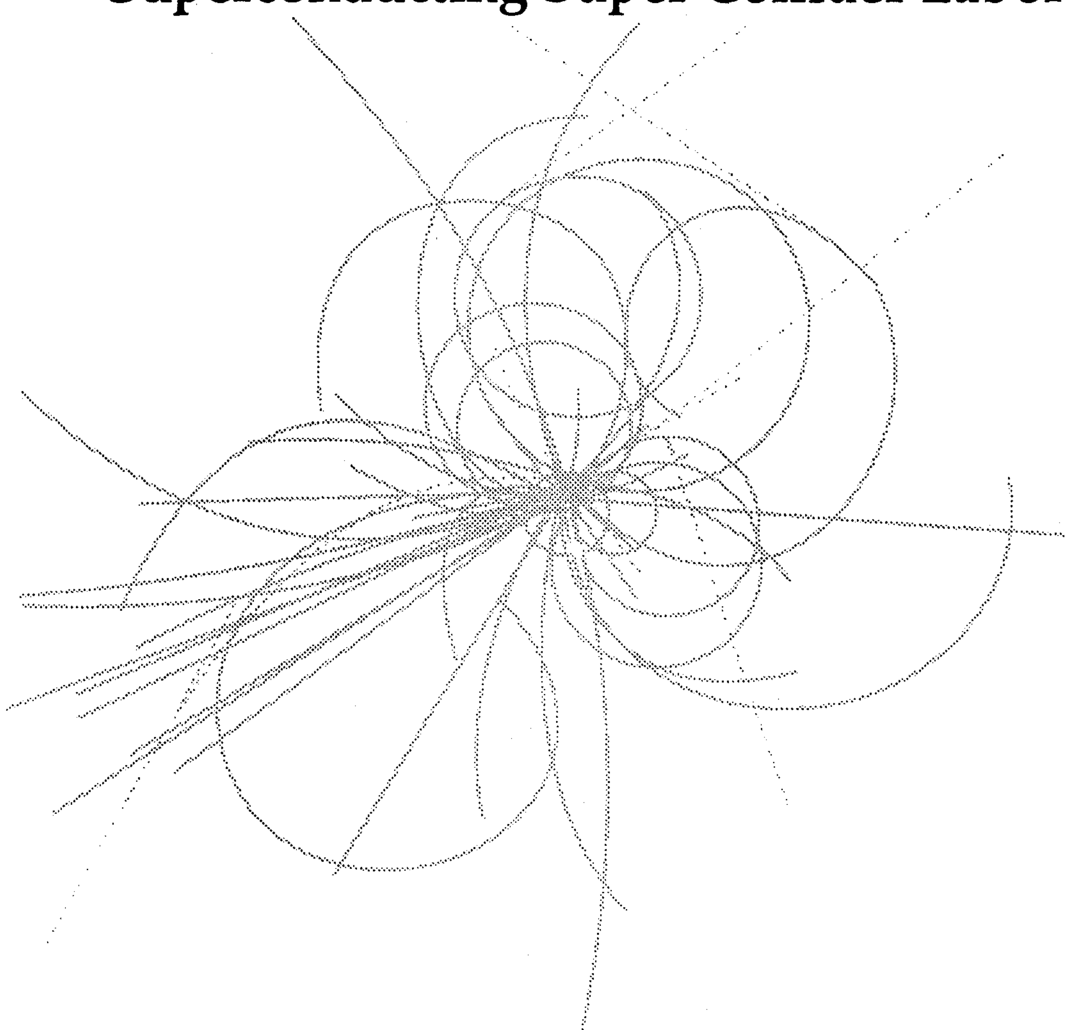

A.C. Losses in the High Energy Booster Dipole Magnets

R. Jayakumar, V. Kovachev, G. Snitchler, and D. Orrell

June 1991

SSCL-490

A.C. Losses in the SSC High Energy Booster Dipole Magnets*

R. Jayakumar, V. Kovachev, G. Snitchler, and D. Orrell

Magnet Systems Division
Superconducting Super Collider Laboratory†
2550 Beckleymeade Ave.
Dallas, TX 75237

June 1991

---

*Presented at the MT-12 Conference, Lenningrad, U.S.S.R., June 24-28, 1991.

†Operated by the Universities Research Association, Inc., for the U.S. Department of Energy under Contract No. DE-AC02-89ER40486.

A.C. Losses in the SSC High Energy Booster Dipole Magnets

R. Jayakumar, V. Kovachev, D. Orrell, and G. Snitchler

Magnet Systems Division
SSC Laboratory*
2550 Beckleymeade Ave., Dallas, TX 75237

Abstract. The baseline design for the SSC High Energy Booster (HEB) has dipole bending magnets with a 50 mm aperture. An analysis of the cryogenic heat load due to A.C. losses generated in the HEB ramp cycle are reported for this magnet. Included in this analysis are losses from superconductor hysteresis, yoke hysteresis, strand eddy currents, and cable eddy currents. The A.C. loss impact of 2.5 μm vs. 6 μm filament conductor is presented. A 60 mm aperture design is also investigated.

INTRODUCTION

The high energy booster dipole magnet (HEBDM) has a different set of operating conditions than those of to the collider dipole magnet (CDM). The current specifications for HEBDM operation involves eight bipolar ramp cycles which provide a continuous heat load due to A.C. losses during injection in to the collider ring.

This heat load must be accurately determined to evaluate the cryogenic performance for a series of magnets. The last magnet in the string before the recooler could have a significant temperature rise; therefore, a significant loss of temperature margin could occur and degrade the machine performance. In this paper, the heat load is estimated from the major sources of A.C. loss: superconductor hysteresis, yoke hysteresis, strand eddy currents, and cable eddy currents.

The HEBDM is specified to have the same design as the CDM, shown in table 1. A conductor containing 2.5 μm filaments is under consideration to reduce A.C. losses and persistent current harmonics. A 60 mm aperture magnet design is also shown in table 1 and the A.C. losses of both designs are estimated in the next section.

Table 1 Designs for HEB Dipole

	50 mm design	60 mm design
conductor:		
inner strands	30	28
inner turns	19	25
outer strands	36	32
outer turns	26	23
sc volume/15m (m^3)	0.0136	0.0138
collar+yoke vol (m^3)	1.25	1.2
oper. field (T)	6.38	5.8
oper. cur (A)	6250	5950
oper. cur. den. (A/mm^2)	1015	1036
saturation %	2.35	1.75
peak field (T)	6.7	6.2
quench current (A)	7270	7310
quench peak field (T)	7.6	7.4
que. cur. den. (A/mm^2) (inner)	1181	1272
quench field (T)	7.27	6.96
MARGIN		
quench field %	13.9	20
quench current %	16.3	22.3
temp. margin (K)	0.75	1.1

* Operated by Universities Research Association, Inc., for the U.S. Department of Energy under Contract No. DE-AC02-89ER40486.

A.C. LOSSES ANALYSIS

The major technical design consideration for the HEBDM is the heat loss due to ramping cycles, usually referred to as A.C. losses. The major sources of A.C. loss are magnetization hysteresis in the superconductor and the yoke, and eddy current losses in the cable volume. It is once again emphasized that the 60 mm design presented is primarily for A.C. loss studies and does not constitute a mature design.

During the HEBDM operations the multifilament conductor is exposed to various values of magnetic field, B, depending on its position in the inner or outer coil of the magnet configuration. To determine precisely the local or average value of B for a particular conductor the magnetic induction distribution for the entire coil volume must be known. This information is also required for determination of the local or average value of critical current density in a particular region of the magnet coils.

The standard bulk magnetization approximation for cylindrical geometry filaments is expressed as

$$M = \frac{2}{3\pi}\mu_o J_c d_f (1 - \frac{J}{J_c}) \tag{1}$$

where d_f is the diameter of the filament, J the current density during the ramp cycle, J_c is the critical current density at a given filament's field and operating temperature, and M is expressed in Tesla. A bulk model for magnetization is justified because the magnetic field fully penetrates the filaments at $B > \mu_o J_c(B) d_f/\pi$. The energy dissipated during a ramp from zero to B_m can be expressed as

$$Q_h^s = \frac{1}{\mu_o}\int_0^{B_m} M dB \tag{2}$$

where B_m is the local maximum field. Two methods have been employed to compute J_c in the conductor and evaluate the integral in equation (2). The first technique involves an analytic formula for the field profile during the ramp cycle and a second technique numerically computes B in the coil volume in an infinite-iron approximation. Also, the more accurate numerical simulations use a J_c surface derived from experimental data.[1]

The analytical approach requires a simple approximation for the critical current density. J_c can be approximated using the Kim-Anderson model[2] as

$$J_c = \frac{J_{co}B_o}{B + B_o} = \frac{2J_c(B_o)B_o}{B + B_o} \tag{3}$$

where J_{co} and B_o represent the characteristics of the material. The local maximum field achieved during a ramp cycle varies within the coil. An approximate estimate of this effect can be obtained by assuming a linear field distribution from B_1 to B_2. By substituting equations (3) and (1) into equation (2) and integrating, we obtain the resulting average heat generation as

$$\begin{aligned}\langle Q_h^s \rangle &= \frac{8}{3\pi} d_f \frac{J_c(B_o)B_o}{B_2 - B_1}\int_{B_1}^{B_2} ln\frac{B_m + B_o}{B_o} dB_m \\ &= \frac{8}{3\pi} d_f \frac{J_c(B_o)B_o^2}{B_2 - B_1}[\frac{B_2 + B_o}{B_o}(ln(\frac{B_2 + B_o}{B_o}) - 1) \\ &- \frac{B_1 + B_o}{B_o}(ln(\frac{B_1 + B_o}{B_o}) - 1)].\end{aligned} \tag{4}$$

The average power loss is

$$\langle W_h^s \rangle = \langle Q_h^s \rangle \frac{\lambda V}{2T_r} \tag{5}$$

where λ is the percentage of superconductor, V is the conductor volume, and $2T_r$ is the ramp period for a complete monopolar cycle.

An estimate of the heat generated during a monocycle for this magnet can be made assuming the following parameters: $d_f = 2.5\mu m$; $B_o = 1$ T; $J_c(B_o) = 10^{10} A/m^2$; $\lambda = 0.4$; $V = 0.0365 m^3$; $2T_r = 100s$; $B_1 = 2$ T; $B_2 = 7$ T. Using equation (5), we obtain the total power loss for both inner and outer conductors due to hysteresis in the superconductor, $\langle W_h^s \rangle = 5.2$ Watts for a magnet length of 15 m and a ramp time of 50 sec. from 0 to full field and ramp down at the same rate. The more accurate numerical solution using an experimental J_c surface and an infinite-iron local magnetic fields gives 3.9 Watts for the same ramp cycle.

In twisted multifilamentary wires, the superconducting filaments are coupled together by changing magnetic field. This coupling causes A.C. losses due to dB/dt related electric field rise along a zig-zag path. The coupling losses are of an eddy current type. Thus the loss per cycle depends on the cycle ramp time, T_r.

To evaluate eddy current coupling losses in the HEBDM multifilamentary conductor strand, we use the anisotropic resistivity model [3]. This model gives the following formulae for the coupled eddy current power losses per unit volume:

$$\frac{W_e}{V} = \frac{\dot{B}_i^2}{\rho_{et}} \left(\frac{L}{2\pi}\right)^2 = \frac{2\dot{B}_i^2}{\mu_o} \tau \tag{6}$$

where $\dot{B}_i$ is the local time derivative of the magnetic field within the composite and the time decay is related to the effective resistivity and pitch length by the formula

$$\tau = \frac{\mu_o}{2\rho_{et}} \left(\frac{L}{2\pi}\right)^2. \tag{7}$$

The time constant, τ, can be estimated from strand magnetization data using the relationship:

$$2\dot{B}\tau = M_e.$$

Using strand data from A. Ghosh[4], with $M_e = 0.3$ mT for a conductor with a copper-to- superconductor ratio $\gamma = 1.5$ and a ramp rate of $\dot{B} = 0.021$ T/sec, a $\tau = 7.1$ msec is obtained.

The second alternative to obtain τ involves estimating the effective transverse resistivity, ρ_{et}, of the eddy current path as

$$\frac{1}{\rho_{et}} = \frac{1}{\rho_t} + \frac{w}{a\rho_m} + \frac{aw}{\rho_m}\left(\frac{2\pi}{L}\right)^2$$

a is the outer filament composite radius and ω is the thickness of the outer copper jacket. From equation (6), the resulting decay time is $\tau = 6.7$ msec. Data for 2.5 μm conductor is unavailable at the time of this report. It is difficult to predict the resistivity of the eddy current path. The 2.5 μm conductor is constructed such that the filaments are sub-bundled. Sub-bundles are separated by a copper matrix which could provide a low resistance path for eddy currents; however, some Cu-Ti compounds could be formed in the matrix which would increase the resistivity.

The eddy current power generated is

$$W_e = \int \tau \frac{2\dot{B}_i^2}{\mu_o} dV \tag{8}$$

where the integral is over the total conductor volume. Two solution techniques are used for the eddy current computation. Both are similar to the hysteresis calculations. In the analytic approximation, the average eddy current effect is approximated assuming a linear B field distribution in the coil volume ranging from B_1 to B_2. The resulting power generation expression is

$$\langle W_e \rangle^{st} = \frac{2V}{3\mu_o} \frac{B_2^3 - B_1^3}{B_2 - B_1} \frac{\tau}{T_r^2} \tag{9}$$

The analytic power expression yields a loss of 3.7 Watts assuming $B_1 = 2$ T and $B_2 = 7$ T. The numerical integration of equation (8) yields 3.4 Watts for the same $2T_r = 100$ seconds ramp cycle with a peak current of 6250 A (6.4T) for a 50 mm HEBDM. A scale law is used to represent the change in γ for the outer cable. The estimate of error in power loss from strand data is of the order of 30%.

Strand-to-strand coupling in cabled conductors occurs when the single strands are not insulated and the contact resistance between them is low enough to achieve significant eddy current paths. The magnetic field induced currents pass across strand-to-strand interfaces causing eddy current type losses.

One method to estimate interstrand losses is to determine the resistance, R, for the particular cable of given conditions emulating the coil conditions. Then using the model proposed by G. Morgan[5] the strand-to-strand coupling losses for superconducting braids are given by

$$W_e^{st} = \frac{N^2 h^2 L \dot{B}^2}{60R} \tag{10}$$

where W_e^{st} is in Watts per unit length of the braid, h is the width of the braid, L is the half braid pitch length, R is the crossover resistance of the braid, and N is the number of strands in the braid. The crossover resistance in the braid (or cable), however, is not directly measurable, since it is difficult to separate a single crossover or a few crossovers from the remainder of the braid. To evaluate interstrand coupling losses for the 50 mm HEBDM conductor we have used the magnetization data obtained by A. Ghosh[4]. These data are based on comparison between the magnetization for a SSC cable with 23 strands stressed with 1.89 Mpa kpsi and the magnetization of the uncabled strands. The comparison shows that any excess magnetization due to interstrand coupling is $2M_e^{st} = 0.2 \pm 0.3$ mT. These measurements were carried out by comparing magnetization at ramp rates of 21 mT/sec and 42 mT/sec. The rather high error in the measurements is related to experimental limitations. However, analytical estimates like the one shown above indicate that a value of 2 $M_e = 0.2$ mT is a reasonable estimate and the upper limit of 0.5 mT is too high. The time constant may be scaled using

$$\tau_{eff}^{st} = \tau_t \left(\frac{h}{h_t}\right)^2 \frac{L}{L_t} \left(\frac{N}{N_t}\right)^2 \tag{11}$$

where h_t is the test cable width, L_t is the test sample half pitch length, and N_t is the test sample number of strands. From this cable test $\tau_t = 2.4$ msec, $h_t = 0.0093$ m, $L_t = 0.0125$ m, and $N_t = 23$. The strand-to-strand eddy current power generated is

$$W_e^{st} = \int \tau^{st} \frac{2\dot{B}_i^2}{\mu_o} dV \tag{12}$$

which is an integral over all cable volume. Assuming a linear field distribution, we obtain

$$\langle W_e^{st} \rangle = \frac{2}{3\mu_o} V(1-\lambda) \frac{B_2^3 - B_1^3}{B_2 - B_1} \frac{\tau^{st}}{T_r^2} \tag{13}$$

The analytic model for the 50 mm HEBDM with 2.5 μm filament conductor gives a $\tau_{eff}^{st} = 9.9$ msec and $\langle W_e^{st} \rangle = 3.4$ Watts.

The only significant τ_{eff}^{st} contribution is from B-field component perpendicular to the cable width. A numerical calculation using local coil perpendicular B-field components for equation (12) yields $W_e^{st} =$ 1.5 Watts. This result is much smaller than the analytic result due to the effect of field orientation, which was not taken into account in the analytical estimate.

The proximity effect can cause a time-independent interfilament coupling when the filament spacing is of the order of the superconducting coherence length. This coupling may produce rather high additional magnetization and hysteresis type losses in the conductors with closely spaced fine filaments and low resistivity normal metal matrix (pure-Cu). In some cases when the filament spacing is small but not enough to cause superconducting tunneling, the proximity effect can reduce the transverse resistivity and unacceptably enhance the standard coupling between the filaments. Estimates made for the 2.5 μm filament HEBDM conductor with a Cu-Mn matrix showed that proximity coupling is neglegible.

Another significant source of heat generation is the irreversible magnetization in ferromagnetic materials. Superconducting accelerator magnets use low carbon steel usually having a coercivity of 0.8 to 3.0 Oe. If the material properties are well known, it is relatively easy to compute the heat generated by integrating the area inside the hysteresis loop:

$$Q = \int_{vol} \int_{cycle} M dB dV \tag{14}$$

The saturation magnetization point is approximately 1.6 T-2.1 T where the loop closes. A small but significant percentage of the iron in a dipole magnet does not reach 1.6 T and therefore forms a smaller hysteresis loop. Finite element saturable iron calculations reveal that between 60- 80% of the yoke is saturated to beyond 1.6 T depending on the design and peak field operating conditions. A weighted contributed volume, V^*, can be estimated from finite element models of yoke saturation

$$W_y = \frac{V^*}{T_r} \int_0^{B_{max}} M dB \tag{15}$$

Results are very dependent on material properties. Since the low temperature coercivity is not currently known, the actual A.C. loss due to yoke hysteresis could be higher than the estimates in this paper. However, measurements on a limited number of materials both at 300 K and 4.2 K suggest that there is little change in coercivity.[6]

The area inside the magnetization loop scales linearly with the coercivity, C, as seen in table (2). Data indicates that the hysteresis area scales as $B^{1.6}$ where B is the peak field seen by the iron. Once low temperature data is available for selected materials, corrections of estimates can be made using this scaling information.

Table 2 Yoke Hysteresis Effects

Material	C Oe	Q/V J/m^3	Q/V/C $J/m^3 - Oe$	W/V* W/m^3
A-36	3.1	1950	630	9.8
Kawasaki	1.25	763	610	3.8
Armco	0.6	336	560	1.7
* evaluated at T_r = 50 sec.				

In conclusion, yoke hysteresis losses scale linearly with the coercivity yielding approximately 600 $J/m^3 - Oe$. Little data is available for temperatures near 4 K and these models use room temperature magnetization data. Clearly, more information is needed for cryogenic temperatures.

It must be pointed out that the yoke hysteresis loss estimated above is applicable only to a bipolar (truly AC) operation. If the magnet were to be operated as a monopolar device, the yoke loss is expected to reduce significantly.

Table (3) provides a summary of power loads for the two magnet designs. These results are based on a ramp time of T_r = 50 sec. without rest period. All hysteresis effects and allowances for rest periods scale as

$$W_h = W_h^{(50)}(\frac{50}{T_r}).$$

The results in this paper represent the impact of a full hysteresis loop. If the area inside the yoke iron hysteresis loop is small for a monopolar operation compared to the bipolar operation this would make a significant impact on cryogenic needs. All eddy current effects are dB/dt dependent and scale as

$$W_e = W_e^{(50)}(\frac{50}{T_r})^2.$$

The time dependence of eddy current losses implies that significant heat load reduction would accompany slower ramp rates.

Table 3 Summary of A.C. Losses

	50 mm design		60 mm design	
	2.5 μm	6.0 μm	2.5 μm	6.0 μm
1.8Tev (5.8T)				
amps	5650	5650	5950	5950
cable hys.	3.9	9.3	3.9	9.3
strand eddy	2.6	2.6	2.7	2.7
cable eddy	1.2	1.2	0.9	0.9
yoke hys.	2.4	2.4	2.4	2.4
Total Watts				
Case 1	10.1	15.5	9.9	15.3
Case 2	8.4	12.9	8.2	12.7
Case 3	3.7	6.2	3.7	6.1
2.0Tev (6.38T)				
amps	6250	6250	6600	6600
cable hys.	3.9	9.3	3.9	9.3
strand eddy	3.2	3.2	3.3	3.3
cable eddy	1.5	1.5	1.0	1.0
yoke hys.	3.1	3.1	3.1	3.1
Total Watts				
Case 1	11.7	17.1	11.3	16.7
Case 2	9.8	14.3	9.4	13.9
Case 3	4.3	6.7	4.2	6.6
Case 1 T_r = 50 sec. with no rest period Case 2 T_r = 50 sec. with 10 sec. rest period Case 3 T_r = 100 sec. with 10 sec. rest period				

The comparisons in table (3) for the 60 mm design and the CDM design are listed for two injection energies. If the injection energy is 2 TeV for both magnets with 6 μm filament conductor, the total A.C. loss for the 60 mm design is 15.3 Watts and for the CDM design is 15.5 Watts. With equivalent operational parameters, these two designs produce approximately the same power.

Preliminary experiments at FNAL[7] show that A.C. losses of a 40 mm design CDM model magnet are in very good agreement with calculations for monopolar operation mode. For instance, the hysteresis losses are estimated to be 64 J and are observed as 66 J. The eddy current losses at 300 A/sec are estimated at 75 J and are observed as 80 J. A comparison of the calculated total hysteresis losses (conductor and yoke) and the experimentally obtained losses for bipolar operation also gives a satisfactory result, 198 J and 188 J respectively. Though this is not evident in ref. [7], it must be noted that a considerable portion of the hysteresis loss increase comes from a much larger iron hysteresis loop area of the bipolar cycle. According to our calculations that increase is approximately 70 J/cycle for the FNAL model magnet, assuming a coercivity of 1.9 Oe and that 85% of the iron is near saturation. The experimental ramp dependent losses are unexpectedly low. Taking into account simple considerations, the eddy current losses must be at least a factor of two larger than for a monopolar cycle. The experimental results, however, are 80 J/cycle and 100 J/cycle for monopolar (50-5000 A at 300 A/sec) and bipolar (-5000-5000 A at 300 A/sec) operation respectively.

Assuming no impact from proximity effects and that eddy current contributions do not vary drastically between 6 μm and 2.5 μm filament conductor, there is a significant difference between the heat loads of these two filament types. The manufacturability of 2.5 μm filament conductor may be a design consideration but, this issue is beyond the scope of this paper.

An estimate of the cryogenic and margin impact has been made using a series of 2-dimensional thermal finite element models and the heat loads presented in table (3). In particular, the 50 sec. ramp up with a 10 sec. rest period has been used and represents peak HEB operation. The results from this model are published in ref. [8].

CONCLUSIONS

The major sources of cryogenic heat load are from hysteresis in the superconductor, hysteresis in the yoke, and eddy currents in the cable. There are a number of uncertainties in determination of A.C. losses of real superconducting magnets. In magnet conductors or cables the critical current density can vary with length due to non-ideal geometry and source technology factors: sausaging, local stress, nonuniformity of cabling, etc. A.C. losses could be also affected by self-welded, touched, or sub-bundled filaments, or by local differences in matrix resistivity due to different deformation history, an incomplete final anealing, or by Cu-Ti formation. As previously discussed, interstrand losses strongly depend on compaction and surface conditions of the wires which can also differ with their length.

Hysteresis losses in the magnet yoke can not be calculated precisely at present due to a lack of information for the properties of low carbon steel near 4.2K. In addition, the precise determination in a magnet may require knowledge of magnetization stress dependence at low temperatures. However, recent manufacturing techniques (e.g. in Armco) have provided low coercivity iron (0.6 Oe) and use of this is contemplated for the HEB after qualification and testing and this could render the yoke loss unimportant.

The models for A.C. loss determination discussed above assume approximations which can have significant effect. For instance A.C. loss evaluation in the vicinity of zero field is rather simplified. Since the critical state model enables the determination of $\nabla \times \vec{B}$ but not $\nabla \times \vec{H}$ (the free current density which is necessary for a loss calculation) it is assumed that $H = B/\mu_o$ which is a very rough approximation for the region near zero field. As known, the reversible magnetization curve for hard type II superconductors can not be theoretically determined or experimentally obtained.

Preliminary experimental results agree well with these calculations. More experiments must be performed to resolve the A.C. losses heat load for HEB design considerations.

Finally, a significant source of energy loss could arise from purely mechanical causes. It is known that the magnet coils have a hysteretic stress-strain curve and the cycling of the coil stresses during ramp cycles could result in the release of frictional energies stored in the stress-strain hysteresis. This effect is known to be very strongly dependent upon details of the magnet, preconditioning and thermal cycling. The analysis in this paper does not include mechanical effects.

The above sources of error and uncertainties will be addressed through a program of experimental measurements and tests. These include a more accurate measurement of strand eddy current magnetization, strand-to-strand coupling effects using cables with a larger number of strands, higher ramp rate, and measurement of iron magnetization at low temperatures. A comprehensive A.C. loss testing program is under way to measure the loss in 50 mm model magnets and this will be supplemented by a long magnet test in the future. The 2.5 μm filament conductor is still an appealing option to reduce A.C. losses although it may be possible to use 6 μm filament conductor.

References

[1] G. Morgan, J. Appl. Phys., 44, 3319 (1973).
[2] V. Kovachev, *Energy Dissipation in Superconducting Materials*, Oxford: Clarendon Press, 1991.
[3] M. Wilson, *Superconducting Magnets*, Oxford: Clarendon Press, 1983, pp. 162-181.
[4] A.K. Ghosh, private communication.
[5] G. Morgan, J. Appl. Phys., 44, 3319 (1973).
[6] A.K. Ghosh and K.E. Robins, "Magnetization Measurement of Low Carbon Steel", Technical Note No. 371, Brookhaven National Laboratory (1982).
[7] M.J. Lamm, J.P. Ozelis, K.J. Coulter, S. Delchamps, T.S. Jeffery, W. Kinney, W. Koska, J. Strait, and M. Wake, "Bipolar and unipolar tests of 1.5m model SSC collider dipole magnets at Fermilab", presented at the Particle Accelerator Conference in San Francisco, May 1991.
[8] B. Aksel, K. Leung, and G. Snitchler, "Evaluation of cooling performances for possible HEB dipole magnets", to be published in an internal SSC report.